This article is made available via the ACS COVID-19 subset for unrestricted RESEARCH re-use and analyses in any form or by any means with acknowledgement of the original source. These permissions are granted for the duration of the World Health Organization (WHO) declaration of COVID-19 as a global pandemic.

ACS NANO

www.acsnano.org

ARTICLE

Aerosol Filtration Efficiency of Common Fabrics Used in Respiratory Cloth Masks

Abhiteja Konda,[⊥] Abhinav Prakash,[⊥] Gregory A. Moss, Michael Schmoldt, Gregory D. Grant, and Supratik Guha*

Cite This: *ACS Nano* 2020, 14, 6339−6347

Read Online

ACCESS | Metrics & More | Article Recommendations | Supporting Information

ABSTRACT: **The emergence of a pandemic affecting the respiratory system can result in a significant demand for face masks. This includes the use of cloth masks by large sections of the public, as can be seen during the current global spread of COVID-19. However, there is limited knowledge available on the performance of various commonly available fabrics used in cloth masks. Importantly, there is a need to evaluate filtration efficiencies as a function of aerosol particulate sizes in the 10 nm to 10 μm range, which is particularly relevant for respiratory virus transmission. We have carried out these studies for several common fabrics including cotton, silk, chiffon, flannel, various synthetics, and their combinations. Although the filtration efficiencies for various fabrics when a single layer was used ranged from 5 to 80% and 5 to 95% for particle sizes of <300 nm and >300 nm, respectively, the efficiencies improved when multiple layers were used and when using a specific combination of different fabrics. Filtration efficiencies of the hybrids (such as cotton−silk, cotton−chiffon, cotton−flannel) was >80% (for particles <300 nm) and >90% (for particles >300 nm). We speculate that the enhanced performance of the hybrids is likely due to the combined effect of mechanical and electrostatic-based filtration. Cotton, the most widely used material for cloth masks performs better at higher weave densities (*i.e.*, thread count) and can make a significant difference in filtration efficiencies. Our studies also imply that gaps (as caused by an improper fit of the mask) can result in over a 60% decrease in the filtration efficiency, implying the need for future cloth mask design studies to take into account issues of "fit" and leakage, while allowing the exhaled air to vent efficiently. Overall, we find that combinations of various commonly available fabrics used in cloth masks can potentially provide significant protection against the transmission of aerosol particles.**

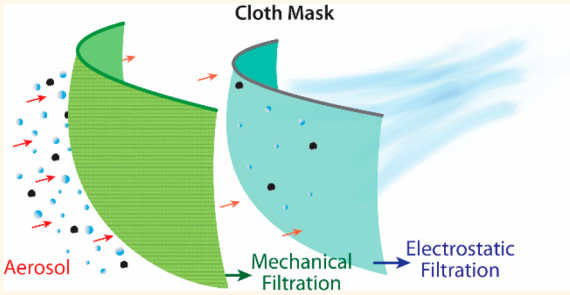

KEYWORDS: *cloth masks, personal protection, aerosols, SARS-CoV-2, face masks, respiratory protection, COVID-19*

The use of cloth masks, many of them homemade,[1,2] has become widely prevalent in response to the 2019−2020 SARS-CoV-2 outbreak, where the virus can be transmitted *via* respiratory droplets.[3−6] The use of such masks is also an anticipated response of the public in the face of future pandemics related to the respiratory tract. However, there is limited data available today on the performance of common cloth materials used in such cloth masks,[7−12] particularly their filtration efficiencies as a function of different aerosol sizes ranging from ∼10 nm to ∼10 μm scale sizes. This is also of current significance as the relative effectiveness of different droplet sizes in transmitting the SARS-CoV-2 virus is not clear, and understanding the filtration response across a large bracketed size distribution is therefore important.[13−16] In this paper, we report the results of experiments where we measure the filtration efficiencies of a number of common fabrics, as well as selective combinations for use as hybrid cloth masks, as a function of aerosol sizes ranging from ∼10 nm to 6 μm. These include cotton, the most widely used fabric in cloth masks, as well as fabric fibers that can be electrostatically charged, such as natural silk.

Respiratory droplets can be of various sizes[17,18] and are commonly classified as aerosols (made of droplets that are <5 μm) and droplets that are greater than 5 μm.[3] Although the fate of these droplets largely depends on environmental factors such as humidity, temperature, *etc.*, in general, the larger droplets settle due to gravity and do not travel distances more than 1−2 m.[19] However, aerosols remain suspended in the air for longer durations due to their small size and play a key role in spreading infection.[14−16] The use of physical barriers such as

Received: April 18, 2020
Accepted: April 21, 2020
Published: April 24, 2020

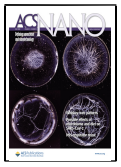

Downloaded via 207.241.229.50 on October 17, 2020 at 09:21:10 (UTC).
See https://pubs.acs.org/sharingguidelines for options on how to legitimately share published articles.

© 2020 American Chemical Society

https://dx.doi.org/10.1021/acsnano.0c03252
ACS Nano 2020, 14, 6339−6347

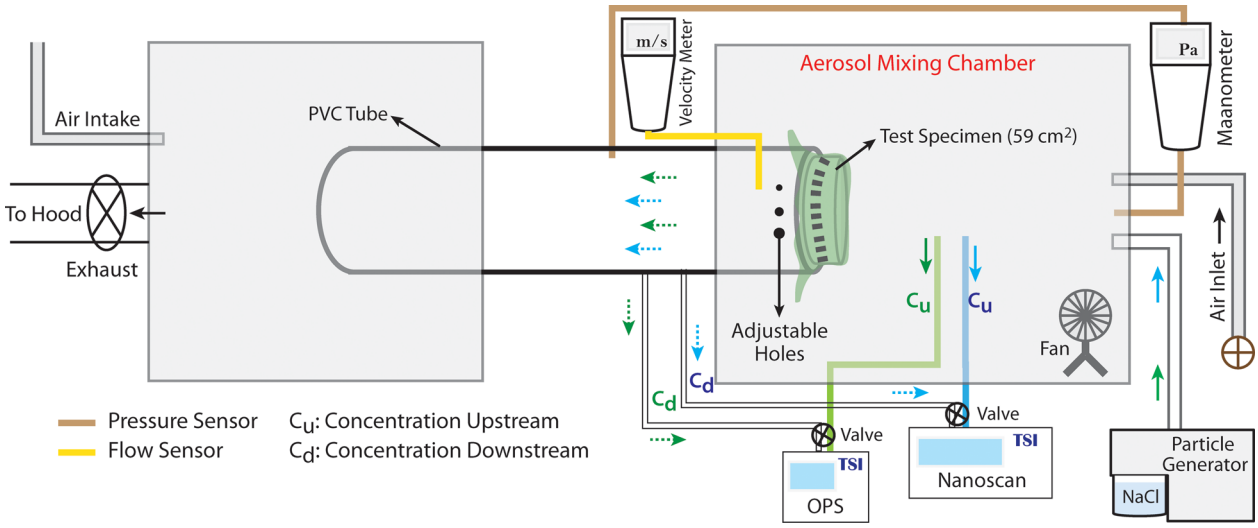

Figure 1. Schematic of the experimental setup. A polydisperse NaCl aerosol is introduced into the mixing chamber, where it is mixed and passed through the material being tested ("test specimen"). The test specimen is held in place using a clamp for a better seal. The aerosol is sampled before (upstream, C_u) and after (downstream, C_d) it passes through the specimen. The pressure difference is measured using a manometer, and the aerosol flow velocity is measured using a velocity meter. We use two circular holes with a diameter of 0.635 cm to simulate the effect of gaps on the filtration efficiency. The sampled aerosols are analyzed using particle analyzers (OPS and Nanoscan), and the resultant particle concentrations are used to determine filter efficiencies.

respiratory masks can be highly effective in mitigating this spread *via* respiratory droplets.[20−22] Filtration of aerosols follows five basic mechanisms: gravity sedimentation, inertial impaction, interception, diffusion, and electrostatic attraction.[23,24] For aerosols larger than ∼1 μm to 10 μm, the first two mechanisms play a role, where ballistic energy or gravity forces are the primary influence on the large exhaled droplets. As the aerosol size decreases, diffusion by Brownian motion and mechanical interception of particles by the filter fibers is a predominant mechanism in the 100 nm to 1 μm range. For nanometer-sized particles, which can easily slip between the openings in the network of filter fibers, electrostatic attraction predominates the removal of low mass particles which are attracted to and bind to the fibers. Electrostatic filters are generally most efficient at low velocities such as the velocity encountered by breathing through a face mask.[25]

There have been a few studies reported on the use of cloth face masks mainly during or after the Influenza Pandemic in 2009;[8−12,26] However, there is still a lack of information that includes (i) the performance of various fabrics as a function of particle size from the nanoscale to the micron sized (particularly important because this covers the ∼10 nm to ∼5 μm size scale for aerosols) and (ii) the effect of hybrid multilayer approaches for masks that can combine the benefits of different filtering mechanisms across different aerosol size ranges.[9,26] These have been the objectives of the experimental work described in this paper. In addition, we also point out the importance of fit (that leads to gaps) while using the face mask.[27,28]

The experimental apparatus (see Figure 1) consists of an aerosol generation and mixing chamber and a downstream collection chamber. The air flows from the generation chamber to the collection chamber through the cloth sample that is mounted on a tube connecting the two chambers. The aerosol particles are generated using a commercial sodium chloride (NaCl) aerosol generator (TSI Particle Generator, model #8026), producing particles in the range of a few tens of nanometers to approximately 10 μm. The NaCl aerosol based testing is widely used for testing face respirators in compliance with the NIOSH 42 CFR Part 84 test protocol.[29,30] Two different particle analyzers are used to determine particle size dimensions and concentrations: a TSI Nanoscan SMPS nanoparticle sizer (Nanoscan, model #3910) and a TSI optical particle sizer (OPS, model #3330) for measurements in the range of 10 to 300 nm and 300 nm to 6 μm, respectively.

Particles are generated upstream of the cloth sample, whose filtration properties are to be tested, and the air is drawn through the cloth using a blower fan which can be controlled in order to vary the airflow rate. Effective area of the cloth sample during the tests was ∼59 cm^2. Measurements of particle size and distribution were made by sampling air at a distance of 7.5 cm upstream and 15 cm downstream of the cloth sample. The differential pressures and air velocities were measured using a TSI digital manometer (model #AXD620) and a TSI Hot Wire anemometer (model #AVM410). The differential pressure (ΔP) across the sample material is an indicator of the comfort and breathability of the material when used as a face mask.[31] Tests were carried out at two different airflows: 1.2 and 3.2 CFM, representative of respiration rates at rest (∼35 L/min) and during moderate exertion (∼90 L/min), respectively.[32]

The effect of gaps between the contour of the face and the mask as caused by an improper fit will affect the efficiency of any face mask.[21,27,28,33] This is of particular relevance to cloth and surgical masks that are used by the public and which are generally not "fitted", unlike N95 masks or elastomeric respirators. A preliminary study of this effect was explored by drilling holes (symmetrically) in the connecting tube onto which the fabric (or a N95 or surgical mask) is mounted. The holes, in proximity to the sample (Figure 1), resulted in openings of area ∼0.5−2% of the active sample area. This, therefore, represented "leakage" of the air around the mask.

Although the detailed transmission specifics of SARS-CoV-2 virus are not well understood yet, droplets that are below 5 μm are considered the primary source of transmission in a respiratory infection,[13,15,34] and droplets that are smaller than

https://dx.doi.org/10.1021/acsnano.0c03252
ACS Nano 2020, 14, 6339−6347

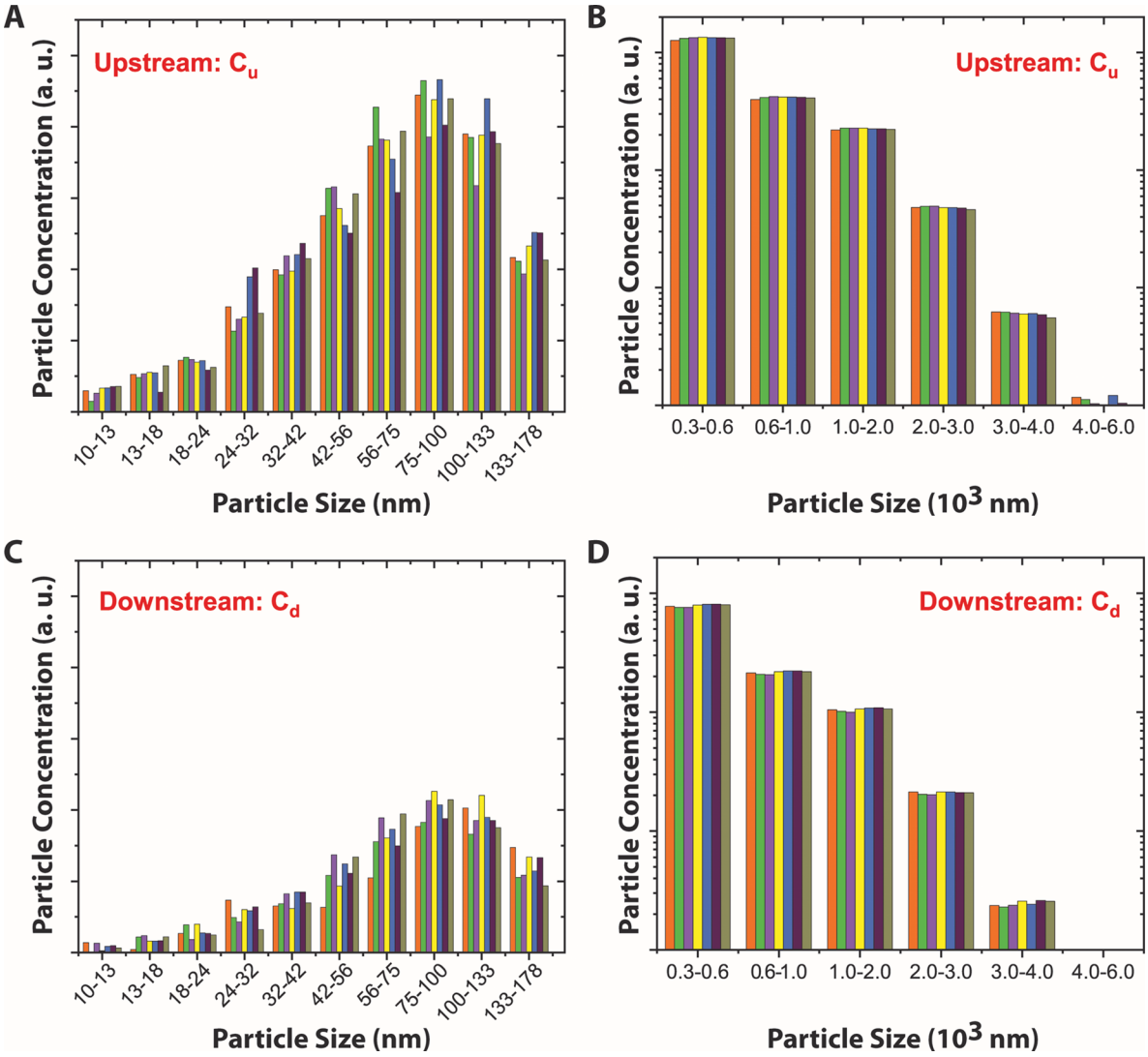

Figure 2. Particle concentration as a function of particle size at a flow rate of 1.2 CFM. Plots showing the particle concentration (in arbitrary units) upstream and downstream through a single layer of natural silk for particle sizes <300 nm (a,c) and between 300 nm and 6 μm (b,d). Each bin shows the particle concentration for at least six trials. The particle concentrations in panels (b) and (d) are given in log scale for better representation of the data. The y-axis scales are the same for panels "a" and "c"; and for panels "b" and "d".

1 μm tend to stay in the environment as aerosols for longer durations of up to 8 h.[19] Aerosol droplets containing the SARS-CoV-2 virus have been shown to remain suspended in air for ∼3 h.[13,35] We have therefore targeted our experimental measurements in the important particle size range between ∼10 nm and 6 μm.

We tested the performance of over 15 natural and synthetic fabrics that included materials such as cotton with different thread counts, silk, flannel, and chiffon. The complete list is provided in the Materials and Methods section. For comparison, we also tested a N95 respirator and surgical masks. Additionally, as appropriate, we tested the efficiency of multiple layers of a single fabric or a combination of multiple fabrics for hybrid cloth masks in order to explore combinations of physical filtering as well as electrostatic filtering.

RESULTS AND DISCUSSION

We determine the filtration efficiency of a particular cloth as a function of particle size (Figure 2) by measuring the concentration of the particles upstream, C_u (Figure 2a,b) and the concentration of the particle downstream, C_d (Figure 2c,d). Concentrations were measured in the size ranges of 10−178 nm (using the nanoscan tool) and 300 nm to 6 μm (using the optical particle sizer tool). The representative example in Figure 2 shows the case for a single layer of silk fabric, where the measurements of C_u and C_d were carried out at a flow rate of 1.2 CFM. Following the procedure detailed in the Materials and Methods section, we then estimated the filtration efficiency of a cloth from C_u and C_d as a function of aerosol particle size.

The results plotted in Figure 3a are the filtration efficiencies for cotton (the most common material used in cloth masks) with different thread counts (rated in threads per inch—TPI—and representative of the coarseness or fineness of the fabric). We compare a moderate (80 TPI) thread count quilter's cotton (often used in do-it-yourself masks) with a high (600 TPI) cotton fabric sample. Additionally, we also measured the transmission through a traditional cotton quilt where two 120 TPI quilter's cotton sheets sandwich a ∼0.5 cm batting (90% cotton−5% polyester−5% other fibers). Comparing the two

https://dx.doi.org/10.1021/acsnano.0c03252
ACS Nano 2020, 14, 6339−6347

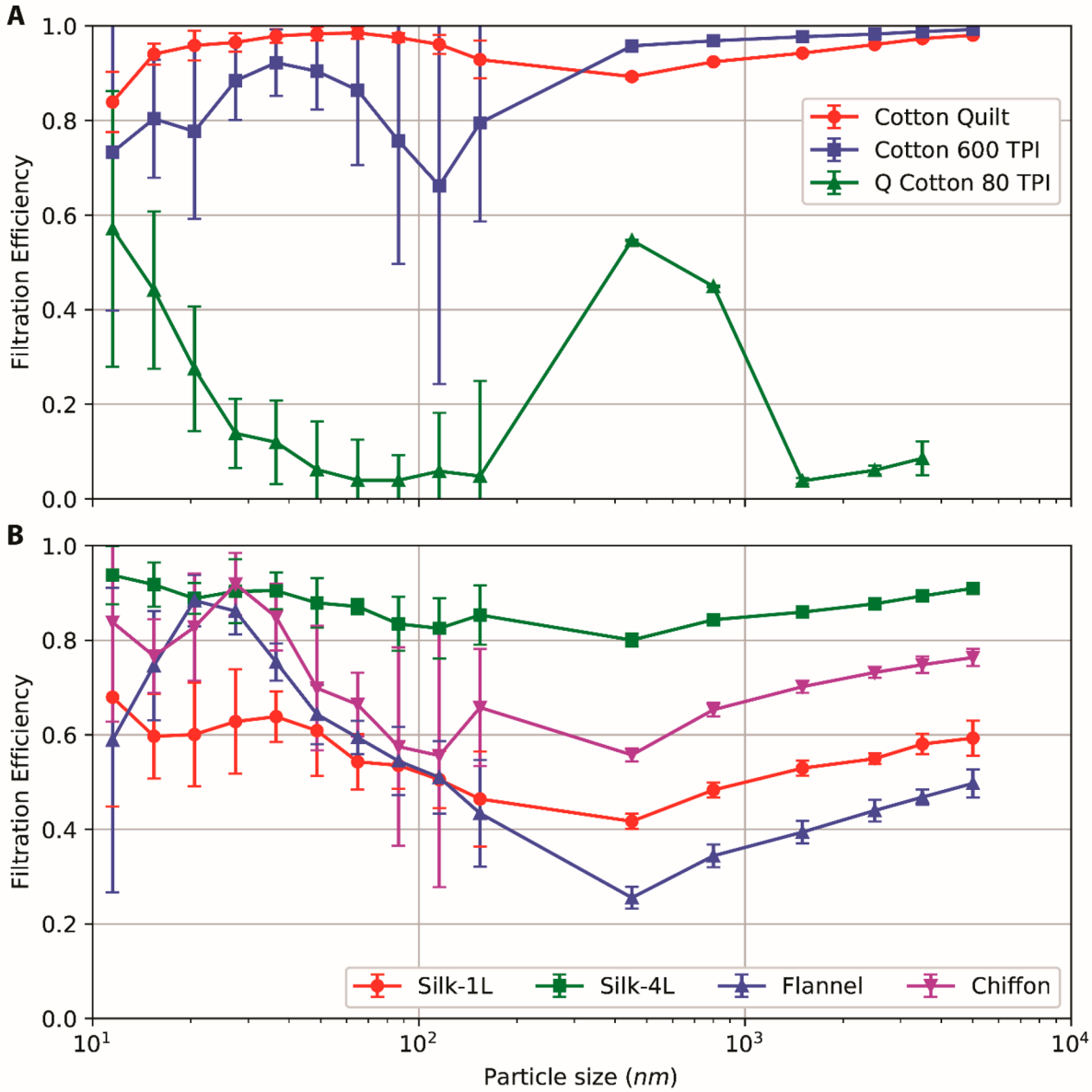

Figure 3. Filtration efficiency of individual fabrics at a flow rate of 1.2 CFM (without gap). (a) Plot showing the filtration efficiencies of a cotton quilt consisting of two 120 threads per inch (TPI) cotton sheets enclosing a ~0.5 cm thick cotton batting, 80 TPI quilters cotton (Q Cotton 80 TPI), and a 600 TPI cotton (cotton 600 TPI). (b) Plot showing the filtration efficiencies of one layer of natural silk (Silk-1L), four layers of natural silk (Silk-4L), one layer of flannel, and one layer of chiffon. The error bars on the <300 nm measurements are higher, particularly for samples with high filtration efficiencies because of the small number of particles generated in this size range, the relatively poorer counting efficiency of the detector at <300 nm particle size, and the very small counts downstream of the sample. The sizes of the error bars for some of the data points (>300 nm) are smaller than the symbol size and hence not clearly visible.

cotton sheets with different thread counts, the 600 TPI cotton is clearly superior with >65% efficiency at <300 nm and >90% efficiency at >300 nm, which implies a tighter woven cotton fabric may be preferable. In comparison, the single-layer 80 TPI cotton does not perform as well, with efficiencies varying from ~5 to ~55% depending on the particle size across the entire range. The quilt, a commonly available household material, with a fibrous cotton batting also provided excellent filtration across the range of particle sizes (>80% for <300 nm and >90% for >300 nm).

Electrostatic interactions are commonly observed in various natural and synthetic fabrics.[36,37] For instance, polyester woven fabrics can retain more static charge compared to natural fibers or cotton due to their lower water adsorption properties.[36] The electrostatic filtering of aerosols have been well studied.[38] As a result, we investigated three fabrics expected to possess moderate electrostatic discharge value: natural silk, chiffon (polyester−Spandex), and flannel (cotton−polyester).[36] The results for these are shown in Figure 3b. In the case of silk, we made measurements through one, two, and four layers of the fabric as silk scarves are often wrapped in multiple layers around the face (the results for two layers of silk are presented in Figure S1 (Supporting Information) and omitted from this figure). In all of these cases, the performance in filtering nanosized particles <300 nm is superior to performance in the 300 nm to 6 μm range and particularly effective below ~30 nm, consistent with the expectations from the electrostatic effects of these materials. Increasing the number of layers (as

https://dx.doi.org/10.1021/acsnano.0c03252
ACS Nano 2020, 14, 6339−6347

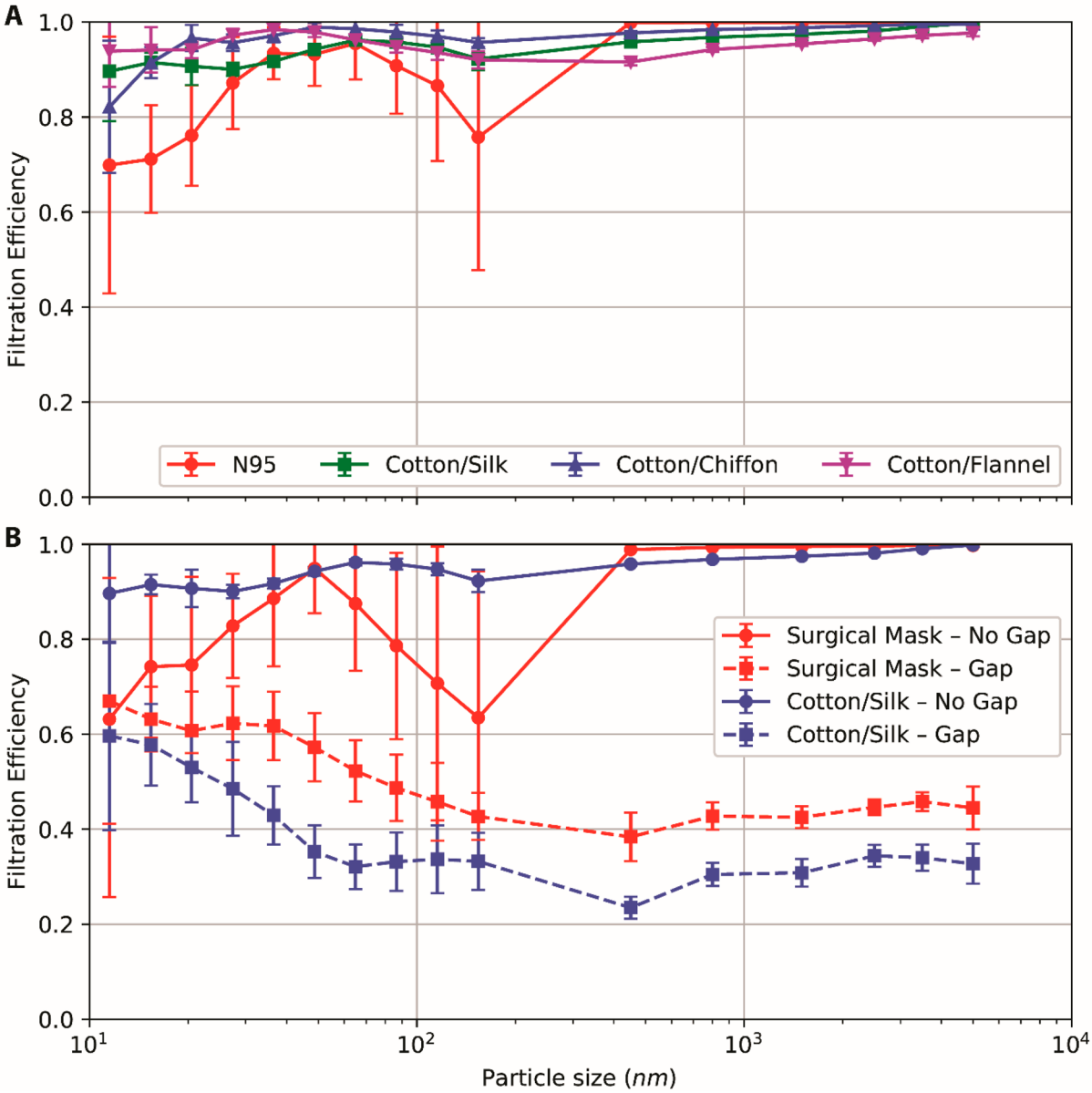

Figure 4. Filtration efficiency of hybrid fabrics at a flow rate of 1.2 CFM. (a) Plot showing the filtration efficiencies without gap for an N95 respirator and a combination of different fabrics: 1 layer of 600 threads per inch (TPI) cotton and 2 layers of silk (cotton/silk), 1 layer of 600 TPI cotton and 2 layers of chiffon (cotton/chiffon), and 1 layer of 600 TPI cotton and 1 layer of flannel (cotton/flannel). (b) Plot showing the filtration efficiencies of a surgical mask and cotton/silk with (dashed) and without a gap (solid). The gap used is ∼1% of the active mask surface area. The error bars on the <300 nm measurements are higher, particularly for samples with high filtration efficiencies because of the small number of particles generated in this size range, the relatively poorer counting efficiency of the detector at <300 nm particle size, and the very small counts downstream of the sample. The sizes of the error bars for some of the data points (>300 nm) are smaller than the symbol size and hence not clearly visible.

shown for silk in Figure 3b), as expected, improves the performance. We performed additional experiments to validate this using the 600 TPI cotton and chiffon (Figure S1). We note that the performance of a four-layer silk composite offers >80% filtration efficiency across the entire range, from 10 nm to 6 μm.

In Figure 4a, we combine the nanometer-sized aerosol effectiveness (for silk, chiffon, and flannel) and wearability (of silk and chiffon because of their sheer nature) with the overall high performance of the 600 TPI cotton to examine the filtration performance of hybrid approaches. We made measurements for three variations: combining one layer 600 TPI cotton with two layers of silk, two layers of chiffon, and one layer of flannel. The results are also compared with the performance of a standard N95 mask. All three hybrid combinations performed well, exceeding 80% efficiency in the <300 nm range, and >90% in the >300 nm range. These cloth hybrids are slightly inferior to the N95 mask above 300 nm, but superior for particles smaller than 300 nm. The N95 respirators are designed and engineered to capture more than 95% of the particles that are above 300 nm,[39,40] and therefore, their underperformance in filtering particles below 300 nm is not surprising.

It is important to note that in the realistic situation of masks worn on the face without elastomeric gasket fittings (such as the commonly available cloth and surgical masks), the

https://dx.doi.org/10.1021/acsnano.0c03252
ACS Nano 2020, 14, 6339−6347

Table 1. Filtration Efficiencies of Various Test Specimens at a Flow Rate of 1.2 CFM and the Corresponding Differential Pressure (ΔP) across the Specimen[a]

	flow rate: 1.2 CFM		
	filter efficiency (%)		pressure differential
sample/fabric	<300 nm average ± error	>300 nm average ± error	ΔP (Pa)
N95 (no gap)	85 ± 15	99.9 ± 0.1	2.2
N95 (with gap)	34 ± 15	12 ± 3	2.2
surgical mask (no gap)	76 ± 22	99.6 ± 0.1	2.5
surgical mask (with gap)	50 ± 7	44 ± 3	2.5
cotton quilt	96 ± 2	96.1 ± 0.3	2.7
quilter's cotton (80 TPI), 1 layer	9 ± 13	14 ± 1	2.2
quilter's cotton (80 TPI), 2 layers	38 ± 11	49 ± 3	2.5
flannel	57 ± 8	44 ± 2	2.2
cotton (600 TPI), 1 layer	79 ± 23	98.4 ± 0.2	2.5
cotton (600 TPI), 2 layers	82 ± 19	99.5 ± 0.1	2.5
chiffon, 1 layer	67 ± 16	73 ± 2	2.7
chiffon, 2 layers	83 ± 9	90 ± 1	3.0
natural silk, 1 layer	54 ± 8	56 ± 2	2.5
natural silk, 2 layers	65 ± 10	65 ± 2	2.7
natural silk, 4 layers	86 ± 5	88 ± 1	2.7
hybrid 1: cotton/chiffon	97 ± 2	99.2 ± 0.2	3.0
hybrid 2: cotton/silk (no gap)	94 ± 2	98.5 ± 0.2	3.0
hybrid 2: cotton/silk (gap)	37 ± 7	32 ± 3	3.0
hybrid 3: cotton/flannel	95 ± 2	96 ± 1	3.0

[a]The filtration efficiencies are the weighted averages for each size range—less than 300 nm and more than 300 nm.

presence of gaps between the mask and the facial contours will result in "leakage" reducing the effectiveness of the masks. It is well recognized that the "fit" is a critical aspect of a high-performance mask.[27,28,33,41] Earlier researchers have attempted to examine this qualitatively in cloth and other masks through feedback on "fit" from human trials.[11,12] In our case, we have made a preliminary examination of this effect *via* the use of cross-drilled holes on the tube holding the mask material (see Figure 1) that represents leakage of air. For example, in Figure 4b, we compare the performance of the surgical mask and the cotton/silk hybrid sample with and without a hole that represents about ∼1% of the mask area. Whereas the surgical mask provides moderate (>60%) and excellent (close to 100%) particle exclusion below and above 300 nm, respectively, the tests carried out with the 1% opening surprisingly resulted in significant drops in the mask efficiencies across the entire size range (60% drop in the >300 nm range). In this case, the two holes were ∼0.635 cm in diameter and the mask area was ∼59 cm^2. Similar trends in efficiency drops are seen in the cotton/silk hybrid sample, as well. Hole size also had an influence on the filtration efficiency. In the case of an N95 mask, increasing hole size from 0.5 to 2% of the cloth sample area reduced the weighted average filtration efficiency from ∼60 to 50% for a particle of size <300 nm. It is unclear at this point whether specific aerodynamic effects exacerbate the "leakage" effects when simulated by holes. Its determination is outside the scope of this paper. However, our measurements at both the high flow (3.2 CFM) and low flow (1.2 CFM) rates show substantial drop in effectiveness when holes are present. The results in Figures 2−4 highlight materials with good performance. Several fabrics were tested that did not provide strong filtration protection (<30%), and examples include satin and synthetic silk (Table S1). The filtration efficiencies of all of the samples that we measured at both 1.2 CFM and 3.2 CFM are detailed in the Supporting Information (Figures S2−S4).

In Table 1, we summarize the key findings from the various fabrics and approaches that we find promising. Average filtration efficiencies (see Materials and Methods section for further detail) in the 10−178 nm and 300 nm to 6 μm range are presented along with the differential pressures measured across the cloths, which represents the breathability and degree of comfort of the masks. The average differential pressure across all of the fabrics at a flow rate of 1.2 CFM was found to be 2.5 ± 0.4 Pa, indicating a low resistance and represent conditions for good breathability (Table 1).[31] As expected, we observed an increase in the average differential pressures for the higher flow rate (3.2 CFM) case (Table S1).

Guidance. We highlight a few observations from our studies for cloth mask design:

Fabric with tight weaves and low porosity, such as those found in cotton sheets with high thread count, are preferable. For instance, a 600 TPI cotton performed better than an 80 TPI cotton. Fabrics that are porous should be avoided.

Materials such as natural silk, a chiffon weave (we tested a 90% polyester−10% Spandex fabric), and flannel (we tested a 65% cotton−35% polyester blend) can likely provide good electrostatic filtering of particles. We found that four layers of silk (as maybe the case for a wrapped scarf) provided good protection across the 10 nm to 6 μm range of particulates.

Combining layers to form hybrid masks, leveraging mechanical and electrostatic filtering may be an effective approach. This could include high thread count cotton combined with two layers of natural silk or chiffon, for instance. A quilt consisting of two layers of cotton sandwiching a cotton−polyester batting also worked well. In all of these cases, the filtration efficiency was >80% for <300 nm and >90% for >300 nm sized particles.

The filtration properties noted in (i) through (iii) pertain to the intrinsic properties of the mask material and do not take into account the effect of air leaks that arise due to improper

https://dx.doi.org/10.1021/acsnano.0c03252
ACS Nano 2020, 14, 6339−6347

"fit" of a mask on the user's face. It is critically important that cloth mask designs also take into account the quality of this "fit" to minimize leakage of air between the mask and the contours of the face, while still allowing the exhaled air to be vented effectively. Such leakage can significantly reduce mask effectiveness and are a reason why properly worn N95 masks and masks with elastomeric fittings work so well.

CONCLUSIONS

In conclusion, we have measured the filtration efficiencies of various commonly available fabrics for use as cloth masks in filtering particles in the significant (for aerosol-based virus transmission) size range of ∼10 nm to ∼6 μm and have presented filtration efficiency data as a function of aerosol particle size. We find that cotton, natural silk, and chiffon can provide good protection, typically above 50% in the entire 10 nm to 6.0 μm range, provided they have a tight weave. Higher threads per inch cotton with tighter weaves resulted in better filtration efficiencies. For instance, a 600 TPI cotton sheet can provide average filtration efficiencies of 79 ± 23% (in the 10 nm to 300 nm range) and 98.4 ± 0.2% (in the 300 nm to 6 μm range). A cotton quilt with batting provides 96 ± 2% (10 nm to 300 nm) and 96.1 ± 0.3% (300 nm to 6 μm). Likely the highly tangled fibrous nature of the batting aids in the superior performance at small particle sizes. Materials such as silk and chiffon are particularly effective (considering their sheerness) at excluding particles in the nanoscale regime (<∼100 nm), likely due to electrostatic effects that result in charge transfer with nanoscale aerosol particles. A four-layer silk (used, for instance, as a scarf) was surprisingly effective with an average efficiency of >85% across the 10 nm −6 μm particle size range. As a result, we found that hybrid combinations of cloths such as high threads-per-inch cotton along with silk, chiffon, or flannel can provide broad filtration coverage across both the nanoscale (<300 nm) and micron scale (300 nm to 6 μm) range, likely due to the combined effects of electrostatic and physical filtering. Finally, it is important to note that openings and gaps (such as those between the mask edge and the facial contours) can degrade the performance. Our findings indicate that leakages around the mask area can degrade efficiencies by ∼50% or more, pointing out the importance of "fit". Opportunities for future studies include cloth mask design for better "fit" and the role of factors such as humidity (arising from exhalation) and the role of repeated use and washing of cloth masks. In summary, we find that the use of cloth masks can potentially provide significant protection against the transmission of particles in the aerosol size range.

MATERIALS AND METHODS

Materials. All of the fabrics used as well as the surgical masks and N95 respirators tested are commercially available. We used 15 different types of fabrics. This included different types of cotton (80 and 600 threads per inch), cotton quilt, flannel (65% cotton and 35% polyester), synthetic silk (100% polyester), natural silk, Spandex (52% nylon, 39% polyester, and 9% Spandex), satin (97% polyester and 3% Spandex), chiffon (90% polyester and 10% Spandex), and different polyester and polyester−cotton blends. Specific information on the composition, microstructure, and other parameters can be found in the Supporting Information (Table S2).

Polydisperse Aerosol Generation. A polydisperse, nontoxic NaCl aerosol was generated using a particle generator and introduced into the mixing chamber along with an inlet for air. The aerosol is then mixed in the mixing chamber with the help of a portable fan. The particle generator produces particles sizes in the ranges of 10 nm to 10 μm.

Detection of Aerosol Particles. The particles were sampled both upstream (C_u, before the aerosol passes through the test specimen) and downstream (C_d, after the aerosol passes through the test specimen) for 1 min. The samples collected from the upstream and downstream are separately sent to the two particle sizers to determine a particle concentration (pt/cc). Each sample is tested seven times following the minimum sample size recommended by the American Industrial Hygiene Association exposure assessment sampling guidelines.[42] We observed a significantly lower particle count in the upper size distribution for both of the data sets, that is, for particles greater than 178 nm for the data from the TSI Nanoscan analyzer and greater than 6 μm for the data from TSI OPS analyzer. We exclude the data above these thresholds for all of the studies reported due to the extremely low counts. We categorize our data based on these two particle analyzers—individually the two plots (Figure 2a,b) show two size distributions—particles smaller than 300 nm and particles larger than 300 nm. Two different flow rates of 1.2 CFM (a face velocity of 0.1 m/s) and 3.2 CFM (a face velocity of 0.26 m/s) were used that corresponded to rates observed at rest to moderate activity, respectively. The velocity of the aerosol stream was measured at ∼5 cm behind where the test specimen would be mounted using a velocity meter.

Differential Pressure. The differential pressure (ΔP) across the test specimen was measured ∼7.5 cm away on either side of the material being tested using a micromanometer. The ΔP value is an estimate of the breathability of the fabric.

Data Analysis. The particle concentrations from seven consecutive measurements were recorded and divided into multiple bins—10 for nanoparticle sizer (dimensions in nm: 10−13, 13−18, 18−24, 24−32, 32−42, 42−56, 56−75, 75−100, 100−133, 133−178) and 6 for optical particle sizer (dimensions in μm: 0.3−0.6, 0.6−1.0, 1.0−2.0, 2.0−3.0, 3.0−4.0, 4.0−6.0). The seven measurements for each bin were subjected to one iteration of the Grubbs' test with a 95% confidence interval to remove at most one outlier per bin. This improves the statistical viability of the data. Following Grubbs' test, average concentrations were used to calculate the filtration efficiencies as described below.

Filtration Efficiency. The filtration efficiency (FE) of different masks was calculated using the following formula:

$$\mathrm{FE} = \frac{C_u - C_d}{C_u}$$

where C_u and C_d are the mean particle concentrations per bin upstream and downstream, respectively. To account for any possible drifts in the aerosol generation, we measured upstream concentrations before and after the downstream measurement and used the average of these two upstream values to calculate C_u (for runs that did not include a gap). We do not measure upstream concentration twice when the run included a gap. The error in FE was calculated using the quadrature rule of error propagation. Due to noise in the measurements, some FE values were below 0, which is unrealistic. As such, negative FE values were removed from consideration in figures and further calculations. In addition to the FE curves, we computed an aggregate filter efficiency for each test specimen. To do this, we took a weighted average of FE values weighted by the bin width for the two particle size ranges (<300 nm and >300 nm). These values are reported in Table 1 and Table S1.

ASSOCIATED CONTENT

Supporting Information

The Supporting Information is available free of charge at https://pubs.acs.org/doi/10.1021/acsnano.0c03252.

Filtration efficiencies for various fabrics tested at two different flow rates and the effect of layering on the filtration efficiencies of chiffon, silk, and 600 TPI cotton; detailed information on various fabrics used (PDF)

https://dx.doi.org/10.1021/acsnano.0c03252
ACS Nano 2020, 14, 6339−6347

AUTHOR INFORMATION

Corresponding Author

Supratik Guha − *Pritzker School of Molecular Engineering, University of Chicago, Chicago, Illinois 60637, United States; Argonne National Laboratory, Lemont, Illinois 60439, United States;* orcid.org/0000-0001-5071-8318; Phone: (914)-325-5147; Email: guha@uchicago.edu

Authors

Abhiteja Konda − *Center for Nanoscale Materials, Argonne National Laboratory, Lemont, Illinois 60439, United States;* orcid.org/0000-0003-3362-0583

Abhinav Prakash − *Center for Nanoscale Materials, Argonne National Laboratory, Lemont, Illinois 60439, United States; Pritzker School of Molecular Engineering, University of Chicago, Chicago, Illinois 60637, United States;* orcid.org/0000-0002-8899-0568

Gregory A. Moss − *Worker Safety & Health Division, Argonne National Laboratory, Lemont, Illinois 60439, United States*

Michael Schmoldt − *Center for Nanoscale Materials and Worker Safety & Health Division, Argonne National Laboratory, Lemont, Illinois 60439, United States*

Gregory D. Grant − *Pritzker School of Molecular Engineering, University of Chicago, Chicago, Illinois 60637, United States*

Complete contact information is available at: https://pubs.acs.org/10.1021/acsnano.0c03252

Author Contributions

⊥A.K. and A.P. contributed equally.

Funding

Department of Defense Vannevar Bush Fellowship Grant No. N00014-18-1-2869.

Notes

The authors declare no competing financial interest.

ACKNOWLEDGMENTS

Use of the Center for Nanoscale Materials, an Office of Science user facility, was supported by the U.S. Department of Energy, Office of Science, Office of Basic Energy Sciences, under Contract No. DE-AC02-06CH11357. S.G. acknowledges the Vannevar Bush Fellowship under the program sponsored by the Office of the Undersecretary of Defense for Research and Engineering [OUSD (R&E)] and the Office of Naval Research as the executive manager for the grant. A.K. acknowledges and thanks Prof. Anindita Basu for helpful discussion and support.

REFERENCES

(1) Ma, N.; Jeffrey, S. S. How to Sew a Fabric Face Mask. *Science* **2020**, *367*, 1424.

(2) Centers for Disease Control and Prevention. Coronavirus Disease 2019 (COVID-19). *Use of Cloth Face Coverings to Help Slow the Spread of COVID-19*; CS316353B, available at https://www.cdc.gov/coronavirus/2019-ncov/prevent-getting-sick/diy-cloth-face-coverings.html, 2020; pp 1−3.

(3) Kutter, J. S.; Spronken, M. I.; Fraaij, P. L.; Fouchier, R. A.; Herfst, S. Transmission Routes of Respiratory Viruses Among Humans. *Curr. Opin. Virol.* **2018**, *28*, 142−151.

(4) Stelzer-Braid, S.; Oliver, B. G.; Blazey, A. J.; Argent, E.; Newsome, T. P.; Rawlinson, W. D.; Tovey, E. R. Exhalation of Respiratory Viruses by Breathing, Coughing, and Talking. *J. Med. Virol.* **2009**, *81*, 1674−1679.

(5) Milton, D. K.; Fabian, M. P.; Cowling, B. J.; Grantham, M. L.; McDevitt, J. J. Influenza Virus Aerosols in Human Exhaled Breath: Particle Size, Culturability, and Effect of Surgical Masks. *PLoS Pathog.* **2013**, *9*, No. e1003205.

(6) National Academies of Sciences. Medicine. *Rapid Expert Consultation on the Possibility of Bioaerosol Spread of SARS-CoV-2 for the COVID-19 Pandemic*; The National Academies Press: Washington, DC, 2020; p 3.

(7) National Academies of Sciences. Medicine. *Rapid Expert Consultation on the Effectiveness of Fabric Masks for the COVID-19 Pandemic*; The National Academies Press: Washington, DC, 2020; p 8.

(8) MacIntyre, C. R.; Seale, H.; Dung, T. C.; Hien, N. T.; Nga, P. T.; Chughtai, A. A.; Rahman, B.; Dwyer, D. E.; Wang, Q. A Cluster Randomised Trial of Cloth Masks Compared With Medical Masks in Healthcare Workers. *BMJ. Open* **2015**, *5*, No. e006577.

(9) Shakya, K. M.; Noyes, A.; Kallin, R.; Peltier, R. E. Evaluating the Efficacy of Cloth Facemasks in Reducing Particulate Matter Exposure. *J. Exposure Sci. Environ. Epidemiol.* **2017**, *27*, 352−357.

(10) Rengasamy, S.; Eimer, B.; Shaffer, R. E. Simple Respiratory Protection–Evaluation of the Filtration Performance of Cloth Masks and Common Fabric Materials Against 20−1000 nm Size Particles. *Ann. Occup. Hyg.* **2010**, *54*, 789−798.

(11) Davies, A.; Thompson, K. A.; Giri, K.; Kafatos, G.; Walker, J.; Bennett, A. Testing the Efficacy of Homemade Masks: Would They Protect in an Influenza Pandemic? *Disaster Med. Public Health Prep.* **2013**, *7*, 413−418.

(12) van der Sande, M.; Teunis, P.; Sabel, R. Professional and Home-Made Face Masks Reduce Exposure to Respiratory Infections Among the General Population. *PLoS One* **2008**, *3*, No. e2618.

(13) van Doremalen, N.; Bushmaker, T.; Morris, D. H.; Holbrook, M. G.; Gamble, A.; Williamson, B. N.; Tamin, A.; Harcourt, J. L.; Thornburg, N. J.; Gerber, S. I.; Lloyd-Smith, J. O.; de Wit, E.; Munster, V. J. Aerosol and Surface Stability of SARS-CoV-2 as Compared With SARS-CoV-1. *N. Engl. J. Med.* **2020**, *382*, 1564.

(14) Morawska, L.; Cao, J. Airborne Transmission of SARS-Cov-2: The World Should Face the Reality. *Environ. Int.* **2020**, *139*, 105730.

(15) Wang, J.; Du, G. COVID-19 May Transmit Through Aerosol. *Ir. J. Med. Sci.* **2020**, 1−2.

(16) Santarpia, J. L.; Rivera, D. N.; Herrera, V.; Morwitzer, M. J.; Creager, H.; Santarpia, G. W.; Crown, K. K.; Brett-Major, D.; Schnaubelt, E.; Broadhurst, M. J.; Lawler, J. V.; Reid, S. P.; Lowe, J. J. Transmission Potential of SARS-CoV-2 in Viral Shedding Observed at the University of Nebraska Medical Center. 2020, *medRxiv*; https://10.1101/2020.03.23.20039446 (accessed 2020-04-04).

(17) Zhang, H.; Li, D.; Xie, L.; Xiao, Y. Documentary Research of Human Respiratory Droplet Characteristics. *Procedia Eng.* **2015**, *121*, 1365−1374.

(18) World Health Organization. Annex C - Respiratory droplets. In *Natural Ventilation for Infection Control in Health-Care Settings*; Atkinson, J., Chartier, Y., Pessoa-Silva, C. L., Jensen, P., Li, Y., Seto, W. H., Eds.; World Health Organization: Geneva, 2009; pp 77−82.

(19) Morawska, L. Droplet Fate in Indoor Environments, or Can We Prevent the Spread of Infection? *Indoor Air* **2006**, *16*, 335−347.

(20) Ching, W.-H.; Leung, M. K. H.; Leung, D. Y. C.; Li, Y.; Yuen, P. L. Reducing Risk of Airborne Transmitted Infection in Hospitals by Use of Hospital Curtains. *Indoor Built Environ.* **2008**, *17*, 252−259.

(21) Lai, A. C. K.; Poon, C. K. M.; Cheung, A. C. T. Effectiveness of Facemasks to Reduce Exposure Hazards for Airborne Infections Among General Populations. *J. R. Soc., Interface* **2012**, *9*, 938−948.

(22) Leung, N. H. L.; Chu, D. K. W.; Shiu, E. Y. C.; Chan, K.-H.; McDevitt, J. J.; Hau, B. J. P.; Yen, H.-L.; Li, Y.; Ip, D. K. M.; Peiris, J. S. M.; Seto, W.-H.; Leung, G. M.; Milton, D. K.; Cowling, B. J. Respiratory Virus Shedding in Exhaled Breath and Efficacy of Face Masks. *Nat. Med.* **2020**, DOI: 10.1038/s41591-020-0843-2.

(23) Hinds, W. C. 9 - Filtration. In *Aerosol Technology: Properties, Behavior, and Measurement of Airborne Particles*, 2nd ed.; John Wiley & Sons: New York, 1999; pp 182−205.

(24) Vincent, J. H. 21 - Aerosol Sample Applications and Field Studies. In *Aerosol Sampling. Science, Standards, Instrumentation and*

Applications; Vincent, J. H., Ed.; John Wiley & Sons: New York, 2007; pp 528−529.
(25) Colbeck, I.; Lazaridis, M. 5 - Filtration Mechanisms. In *Aerosol Science: Technology and Applications*, 1st ed.; Colbeck, I., Lazaridis, M., Eds.; John Wiley & Sons: New York, 2014; pp 89−118.
(26) Jung, H.; Kim, J.; Lee, S.; Lee, J.; Kim, J.; Tsai, P.; Yoon, C. Comparison of Filtration Efficiency and Pressure Drop in Anti-Yellow Sand Masks, Quarantine Masks, Medical Masks, General Masks, and Handkerchiefs. *Aerosol Air Qual. Res.* **2014**, *14*, 991−1002.
(27) Holton, P. M.; Tackett, D. L.; Willeke, K. Particle Size-Dependent Leakage and Losses of Aerosols in Respirators. *Am. Ind. Hyg. Assoc. J.* **1987**, *48*, 848−854.
(28) Rengasamy, S.; Eimer, B. C. Nanoparticle Penetration Through Filter Media and Leakage Through Face Seal Interface of N95 Filtering Facepiece Respirators. *Ann. Occup. Hyg.* **2012**, *56*, 568−580.
(29) Rengasamy, S.; Zhuang, Z.; Niezgoda, G.; Walbert, G.; Lawrence, R.; Boutin, B.; Hudnall, J.; Monaghan, W. P.; Bergman, M.; Miller, C.; Harris, J.; Coffey, C. A Comparison of Total Inward Leakage Measured Using Sodium Chloride (NaCl) and Corn Oil Aerosol Methods for Air-Purifying Respirators. *J. Occup. Environ. Hyg.* **2018**, *15*, 616−627.
(30) Electronic Code of Federal Regulations (eCFR), Title 42: Public Health, Part 84—Approval of Respiratory Protective Devices. *Code of Federal Regulations*, April 2020.
(31) Lord, J. 35—The Determination of the Air Permeability of Fabrics. *J. Text. I.* **1959**, *50*, T569−T582.
(32) Silverman, L.; Lee, G.; Plotkin, T.; Sawyers, L. A.; Yancey, A. R. Air Flow Measurements on Human Subjects With and Without Respiratory Resistance at Several Work Rates. *AMA Arch. Ind. Hyg. Occup. Med.* **1951**, *3*, 461−478.
(33) Grinshpun, S. A.; Haruta, H.; Eninger, R. M.; Reponen, T.; McKay, R. T.; Lee, S.-A. Performance of an N95 Filtering Facepiece Particulate Respirator and a Surgical Mask During Human Breathing: Two Pathways for Particle Penetration. *J. Occup. Environ. Hyg.* **2009**, *6*, 593−603.
(34) Wells, W. F. Airborne Contagion and Air Hygiene: An Ecological Study of Droplet Infections. *J. Am. Med. Assoc.* **1955**, *159*, 90.
(35) Huang, H.; Fan, C.; Li, M.; Nie, H.-L.; Wang, F.-B.; Wang, H.; Wang, R.; Xia, J.; Zheng, X.; Zuo, X.; Huang, J. COVID-19: A Call for Physical Scientists and Engineers. *ACS Nano* **2020**, DOI: 10.1021/acsnano.0c02618.
(36) Perumalraj, R. Characterization of Electrostatic Discharge Properties of Woven Fabrics. *J. Textile Sci. Eng.* **2015**, *06*, 1000235.
(37) Frederick, E. R. Fibers, Filtration and Electrostatics - A Review of the New Technology. *J. Air Pollut. Control Assoc.* **1986**, *36*, 205−209.
(38) Sanchez, A. L.; Hubbard, J. A.; Dellinger, J. G.; Servantes, B. L. Experimental Study of Electrostatic Aerosol Filtration at Moderate Filter Face Velocity. *Aerosol Sci. Technol.* **2013**, *47*, 606−615.
(39) Bałazy, A.; Toivola, M.; Adhikari, A.; Sivasubramani, S. K.; Reponen, T.; Grinshpun, S. A. Do N95 Respirators Provide 95% Protection Level Against Airborne Viruses, and How Adequate are Surgical Masks? *Am. J. Infect. Control* **2006**, *34*, 51−57.
(40) Balazy, A.; Toivola, M.; Reponen, T.; Podgorski, A.; Zimmer, A.; Grinshpun, S. A. Manikin-Based Performance Evaluation of N95 Filtering-Facepiece Respirators Challenged With Nanoparticles. *Ann. Occup. Hyg.* **2005**, *50*, 259−269.
(41) National Academies of Sciences. Medicine. *Reusable Elastomeric Respirators in Health Care: Considerations for Routine and Surge Use*; The National Academies Press: Washington, DC, 2019; p 226.
(42) Bullock, W. H.; Ignacio, J. S. *A Strategy for Assessing and Managing Occupational Exposures*; AIHA Press, American Industrial Hygiene Association, 2006.

NOTE ADDED AFTER ASAP PUBLICATION

The units in Figure 2 were corrected April 27, 2020.

https://dx.doi.org/10.1021/acsnano.0c03252
ACS Nano 2020, 14, 6339−6347